Orientational effects in the excitation and de-excitation of single molecules interacting with donut-mode laser beams

Peter Dedecker[1], Benoît Muls[2], Johan Hofkens[1], Jörg Enderlein[3], and Jun-ichi Hotta[1]

[1]*Department of Chemistry, Katholieke Universiteit Leuven, Celestijnenlaan 200F, 3001 Heverlee, Belgium*

[2]*Department of Chemistry, Université Catholique de Louvain, Place L. Pasteur 1, 1348 Louvain-La-Neuve, Belgium*

[3]*Institute for Biological Information Processing I, Forschungszentrum Jülich, D-52425 Jülich, Germany*

j.enderlein@fz-juelich.de, junichi.hotta@chem.kuleuven.be

Abstract: The interactions between single molecules and three-dimensional donut modes in fluorescence microscopy are discussed based on the vector diffraction theory of light. We find that the use of donut modes generated from a linearly polarized laser beam can yield information about the orientation of immobilized single molecules, allowing for their use in orientational imaging. While fairly insensitive over a range of orientations, this technique is seen to be very sensitive for the subset of orientations where the transition dipole of the molecule is oriented close to the optical axis of the microscope and perpendicular to the input polarization. In a second part of the paper we discuss the impact of the molecular orientation on the resolution improvement in STED microscopy. We find that, even for circularly polarized excitation light, the expected resolution improvement depends on the orientation of the molecule relative to the optical axis of the microscope.

OCIS codes: 180.0180 (Microscopy); 180.2520 (Fluorescence microscopy); 140.3300 (Laser beam shaping); 100.6640 (Superresolution)

References and links

1. T. Klar, S. Jakobs, M. Dyba, A. Egner, and S. Hell, "Fluorescence microscopy with diffraction resolution barrier broken by stimulated emission," Proc. Natl. Acad. Sci. U. S. A. **97**, 8206–8210 (2000).
2. A. Mair, A. Vaziri, G. Weihs, and A. Zeilinger, "Entanglement of the orbital angular momentum states of photons," Nature **412**, 313–316 (2001).
3. D. Zhang and X. Yuan, "Optical doughnut for optical tweezers," Opt. Lett. **28**, 740–742 (2003).
4. P. Rodrigo, V. Daria, and J. Gluckstad, "Real-time interactive optical micromanipulation of a mixture of high- and low-index particles," Opt. Express. **12**, 1417–1425 (2004).
5. J. Hotta, H. Uji-i, and J. Hofkens, "The fabrication of a thin, circular polymer film based phase shaper for generating doughnut modes," Opt. Express **14**, 6273–6278 (2006).
6. D. Ganic, X. Gan, and M. Gu, "Focusing of doughnut laser beams by a high numerical-aperture objective in free space," Opt. Express. **11**, 2747–2752 (2003).
7. K. Youngworth and T. Brown, "Focusing of high numerical aperture cylindrical-vector beams," Opt. Express. **7**, 77–87 (2000).
8. R. Dorn, S. Quabis, and G. Leuchs, "Sharper focus for a radially polarized light beam," Phys. Rev. Lett. **91**, 233,901 (2003).
9. T. Hirayama, Y. Kozawa, T. Nakamura, and S. Shunichi, "Generation of a cylindrically symmetric, polarized laser beam with narrow linewidth and fine tunability," Opt. Express. **14**, 12,839–12,845 (2006).

#79032 - $15.00 USD Received 16 January 2007; revised 28 February 2007; accepted 28 February 2007

10. S. Hell, "Toward fluorescence nanoscopy," Nat. Biotechnol. **21**, 1347–1355 (2003).
11. M. Hofmann, C. Eggeling, S. Jakobs, and S. Hell, "Breaking the diffraction barrier in fluorescence microscopy at low light intensities by using reversibly photoswitchable proteins," Proc. Natl. Acad. Sci. U. S. A. **102**, 17,565–17,569 (2005).
12. B. Sick, B. Hecht, U. Wild, and L. Novotny, "Probing confined fields with single molecules and vice versa," J. Microscop.-Oxf. **202**, 365–373 (2001).
13. E. Wolf, "Electromagnetic diffraction in optical systems I. An integral representation of the image field," Proc. R. Soc. Lond. A **253**, 349–357 (1959).
14. B. Richards and E. Wolf, "Electromagnetic diffraction in optical systems II. Structure of the image field in an aplanatic system," Proc. R. Soc. Lond. A **253**, 358–379 (1959).
15. C. Sheppard and T. Wilson, "The image of a single point in microscopes of large numerical aperture," Proc. R. Soc. A **379**, 145–158 (1982).
16. J. Enderlein, T. Ruckstuhl, and S. Seeger, "Highly efficient optical detection of surface-generated fluorescence," Appl. Opt. **38**, 724–732 (1999).
17. A. Bartko and R. Dickson, "Imaging three-dimensional single molecule orientations," J. Phys. Chem. B. **103**, 11,237–11,241 (1999).
18. T. Ha, T. Enderle, D. Chemla, P. Selvin, and S. Weiss, "Single molecule dynamics studied by polarization modulation," Phys. Rev. Lett. **77**, 3979–3982 (1996).
19. T. Ha, T. Laurence, D. Chemla, and S. Weiss, "Polarization spectroscopy of single fluorescent molecules," J. Phys. Chem. B. **103**, 6839–6850 (1999).
20. J. Jasny and J. Sepiol, "Single molecules observed by immersion mirror objective. A novel method of finding the orientation of a radiating dipole," Chem. Phys. Lett. **273**, 439–443 (1997).
21. J. Sepiol, J. Jasny, J. Keller, and U. Wild, "Single molecules observed by immersion mirror objective. The orientation of terrylene molecules via the direction of its transition dipole moment," Chem. Phys. Lett. **273**, 444–448 (1997).
22. M. Böhmer and J. Enderlein, "Orientation imaging of single molecules by wide-field epifluorescence microscopy," J. Opt. Soc. Am. B. **20**, 554–559 (2003).
23. D. Patra, I. Gregor, and J. Enderlein, "Image analysis of defocused single-molecule images for three-dimensional molecule orientation studies," J. Phys. Chem. A. **108**, 6836–6841 (2004).
24. M. Lieb, J. Zavislan, and L. Novotny, "Single-molecule orientations determined by direct emission pattern imaging," J. Opt. Soc. Am. B. **21**, 1210–1215 (2004).
25. B. Sick, B. Hecht, and L. Novotny, "Orientational imaging of single molecules by annular illumination," Phys. Rev. Lett. **85**, 4482–4485 (2000).
26. L. Novotny, M. Beversluis, K. Youngworth, and T. Brown, "Longitudinal field modes probed by single molecules," Phys. Rev. Lett. **86**, 5251–5254 (2001).
27. S. Hell and J. Wichmann, "Breaking the diffraction resolution limit by stimulated emission: stimulated-emission-depletion fluorescence microscopy," Opt. Lett. **19**, 780–782 (1994).
28. G. Donnert, J. Keller, R. Medda, M. Andrei, S. Rizzoli, R. Lührmann, R. Jahn, C. Eggeling, and S. Hell, "Macromolecular-scale resolution in biological fluorescence microscopy," Proc. Natl. Acad. Sci. U. S. A. **103**, 11,440–11,445 (2006).
29. G. Donnert, C. Eggeling, and S. Hell, "Major signal increase in fluorescence microscopy through dark-state relaxation," Nat. Methods. **4**, 81–86 (2007).
30. V. Westphal, L. Kastrup, and S. Hell, "Lateral resolution of 28 nm (lambda/25) in far-field fluorescence microscopy," Appl. Phys. B. **77**, 377–380 (2003).
31. P. Török and P. Munro, "The use of Gauss-Laguerre vector beams in STED microscopy," Opt. Express. **12**, 3605–3617 (2004).
32. M. Dyba, J. Keller, and S. Hell, "Phase filter enhanced STED-4Pi fluorescence microscopy: theory and experiment," New. J. Phys. **7**, 134 (2005).
33. J. Enderlein, E. Toprak, and P. Selvin, "Polarization effect on position accuracy of fluorophore localization," Opt. Express. **14**, 8111–8120 (2006).

1. Introduction

In the past several years the manipulation of the wave front of a laser beam has become the focus of intense research. An interesting topic in this respect is the creation of laser beams that lead to sharp, zero-intensity 'holes' surrounded by regions of intense illumination when focused. A spatial intensity distribution with a sharp zero at the focus point is often called a 'donut mode', and these modes attract a considerable amount of attention as they can be used to achieve a sub-diffraction limit resolution in optical microscopy when used in combination with a second, unmodified, laser beam [1]. Other applications have been demonstrated as well [2, 3, 4]. Several

#79032 - $15.00 USD Received 16 January 2007; revised 28 February 2007; accepted 28 February 2007

strategies for generating donut modes have been proposed, including the use of circular π-phase shapers [1, 5], and the use of Laguerre-Gaussian [6] or axially-symmetrically polarized [7, 8, 9] laser beams.

In fluorescence microscopy these donut modes can be used in several ways. One way is to excite an ensemble of molecules directly, so that the excited-state distribution resembles a donut shape. Alternatively the light from the donut mode can be used to deactivate molecules in the excited state shortly after the excitation of the sample by another laser beam, through stimulated emission, or to deactivate molecules through the formation of 'dark states' (e.g.; by making use of fluorescence photoswitching).

Because this deactivation or 'dumping' occurs only in the region surrounding the sharp intensity zero, donut modes can be used in the realization of superresolution microscopy by making use of reversible, saturable optical transitions (RESOLFT) [10, 11]. In stimulated-emission depletion (STED) microscopy [1] the quenching of the fluorescence is achieved by red-shifting the donut-mode laser to the red part of the emission band of the dye, leading to stimulated emission, while the molecules in the central 'hole' region are left to fluoresce spontaneously.

In many applications the effect of the donut mode irradiation is considered to be entirely determined by the spatial distribution of the light intensity. While this is obviously a fundamentally important parameter, the light distribution at any point in space is characterized not only by its amplitude but also by its polarization. In general this polarization depends on the input polarization and the position in space relative to the center of the focus.

Most dyes in practical use are characterized by a well-defined transition dipole moment, which is the direction along which the excitation or quenching light is preferentially absorbed. This underlines the importance of the light polarization, and the net result is that the effect of donut mode illumination on a given molecule will depend not only on its position relative to the center of the donut, but also on its orientation. In this paper we wish to examine the effect that this polarization dependence has on the resolution increase that can be obtained in STED microscopy, and whether this dependence can be used for orientational imaging. While these topics might seem only mildly related at first sight, we will find that the same orientational dependence required for the determination of the molecular orientation also has a significant effect on the imaging resolution in STED microscopy. To this end we make use of a combination of theoretical calculations supported by experimental measurements on a sample consisting of individual phenoxy-substituted terylenediimide (TDI) molecules dispersed in a polymethylmethacrylate (PMMA) matrix, which leads to their translational and rotational immobilization. As single molecules can be regarded as ideal dipole absorbers and emitters [12], these molecules can then be used as probes for the local electric field imposed by the donut-mode laser beam.

2. Materials and methods

The phase shaper that was used for the experimental generation of the donut mode was fabricated according to the procedure described in Ref. [5]. Briefly, a thin circular polymer film was prepared on a glass slide and placed into the beam of a helium-neon laser emitting at 633 nm. The thickness and size of the polymer film were chosen such that it induced a π retardation of the wavefront in the central part of the laser beam. This modified beam was then introduced into an Olympus IX70 confocal microscope, where it was focused into a donut mode using an Olympus 100$\times$ NA 1.3 oil immersion objective. The excitation power at the sample was 7.3 μW, and the same objective was used to collect the fluorescence emission, which was detected using a Perkin-Elmer SPCM-AQR-14 avalanche photodiode. Appropriate optical filters were selected to remove the remaining excitation light.

As was mentioned previously, the sample consisted of a film of phenoxy-substituted

#79032 - $15.00 USD Received 16 January 2007; revised 28 February 2007; accepted 28 February 2007

terylenediimide (TDI) molecules dispersed in a PMMA matrix at single-molecule concentrations, spincoated on carefully cleaned coverglasses. These coverglasses were placed onto a piezo-scanning stage (Physike Instrumente), which was used to obtain fluorescence scanning images. For these images the bin-time for each pixel was 5 ms or 10 ms, and the imaged areas were 10 μm $\times$ 10 μm or 2 μm $\times$ 2 μm.

The theoretical calculations were based on the vector-wave optical theory as developed by Richards and Wolf in Ref. [13, 14]. In calculating the orientational imaging we adopted the following parameter values of the focusing oil-immersion objective: numerical aperture NA = 1.3, focal distance 1.8 mm resulting in a back aperture diameter of the objective of 4.68 mm. The refractive index of the immersion oil was assumed to be 1.51, and the excitation wavelength was set to 633 nm. The diameter of the laser beam entering the back aperture of the objective was set to 5 mm (slightly overfilling the back aperture for achieving nearly diffraction-limited focusing), and the phase plate diameter was set to 2.95 mm.

For the STED simulations we assumed plane-wave excitation, which is equivalent to a strongly overfilled back aperture of the objective, and corresponds to diffraction-limited focusing. In these calculations the diameter of the phase plate was set to 3.33 mm, k_{de-act} was set to 0.2 ns^{-1}, while k_{STED} was defined relative to k_{STED}^{sat}, as discussed in the text. The STED pulse was assumed to have a square shape, with a duration of 100 ps. The wavelengths of the excitation laser and the donut-mode laser were chosen to be 488 and 633 nm, respectively.

3. Results and discussion

3.1. Orientational imaging

In general the probability that a molecule will absorb a given photon is proportional to $\cos^2\phi$, where ϕ is the angle between the transition dipole moment of the molecule and the polarization of the photon. If we consider a donut-like spatial distribution of the excitation light in the focus then this relation leads to a rather complex picture, as the transition probability depends not only on the position of the molecule relative to the center of the donut, but also on its orientation. As such we expect the excitation or quenching probability distribution of a single dipole absorber to deviate from the ideal circularly symmetric donut mode intensity distribution.

This is experimentally verified in Fig. 1, where experimentally measured fluorescence images of single molecules are displayed. For the acquisition of these images the Gaussian beam of the linearly polarized excitation laser was modulated into a donut mode and scanned over the sample, while recording the fluorescence emission at every position. The sample molecules were immobilized in such a way as to prevent rotation, so that they function as probes for the intensity distribution and polarization of the excitation light. In general the resulting images show different patterns for each molecule, depending on the orientation of its molecular transition dipole moment.

This finding suggested that linearly polarized excitation light in a donut mode can be used to obtain information on the molecular orientation of single molecules. In an attempt to quantify this phenomenon we devised a set of calculations, in which we determined the polarization of the electric field in the donut mode at every position and calculated the magnitude of the electric field component parallel to a given dipole orientation. A comparison between some experimentally measured and calculated images is shown in Fig. 2, while the results from the calculations are summarized in Fig. 3. In both of these figures θ denotes the out-of-plane angle between the molecular transition dipole and the optical axis of the microscope, while ϕ is the in-plane angle between the excitation polarization and the transition dipole (the polarization of the input laser beam is taken to be along the *x*-axis).

In some cases this polarization dependence leads to strong deviations from the intuitively expected circular symmetry, as can be seen in Fig. 2. For example, a molecule with its transition

#79032 - $15.00 USD Received 16 January 2007; revised 28 February 2007; accepted 28 February 2007

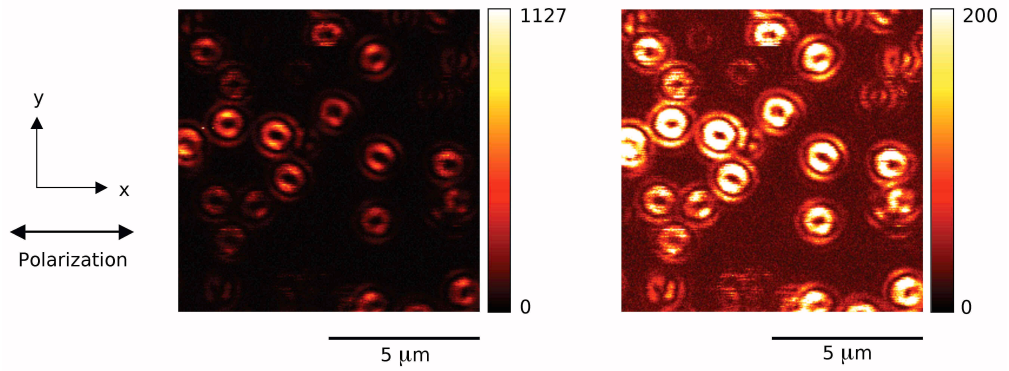

Fig. 1. An experimental fluorescence scanning image for rotationally immobilized single TDI molecules in a PMMA matrix, with two different color scalings. Patterns of differing shapes and intensities are clearly visible.

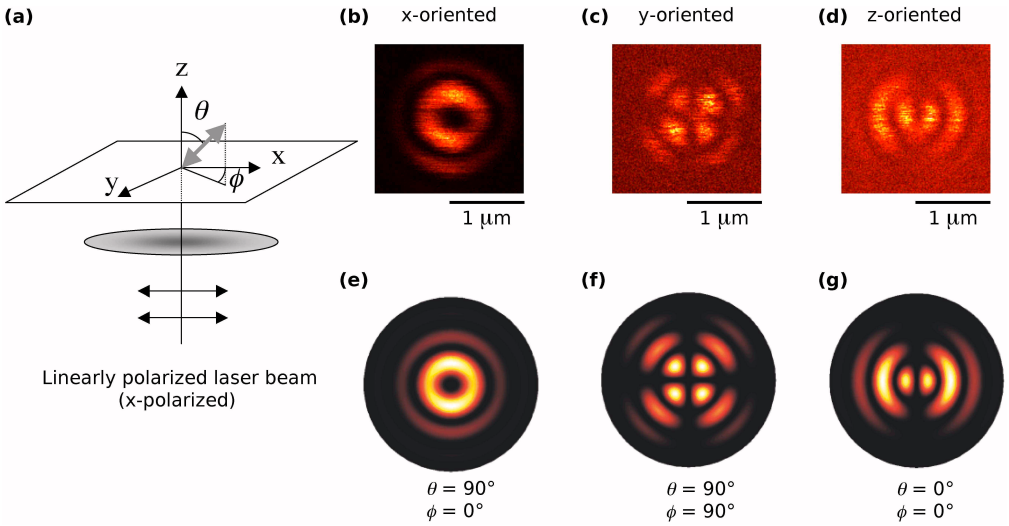

Fig. 2. (a) The coordinate system used for defining the molecular orientation, where the shaded double arrow indicates the molecular transition dipole moment. (b–d) Experimentally obtained scanning images of single TDI molecules with different orientations, and (e–g) comparison with theoretically calculated patterns.

#79032 - $15.00 USD Received 16 January 2007; revised 28 February 2007; accepted 28 February 2007

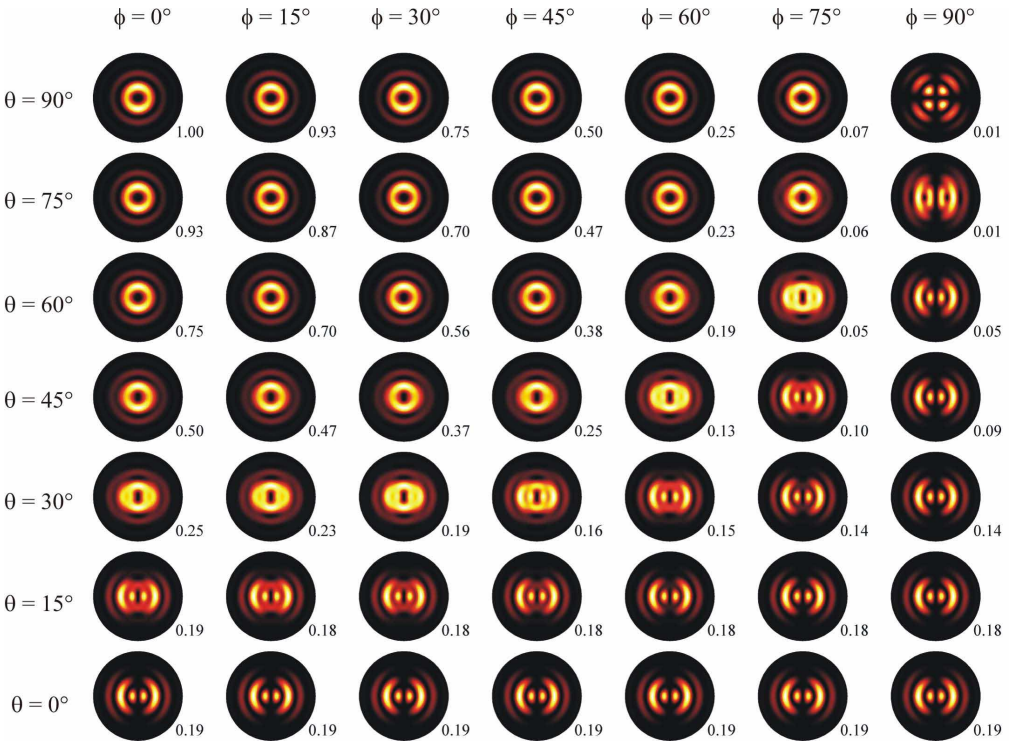

Fig. 3. Simulated fluorescence distributions for single molecules at different molecular orientations, using a linearly polarized donut-mode laser beam as the excitation source. The bright parts of the image are the positions with the most intense dipole interaction (where the molecule is most likely to absorb a photon). The values listed next to the images refer to the maximum observable fluorescence emission for that orientation, relative to that of an *x*-oriented molecule.

dipole moment oriented along the optical axis of the microscope ($\theta = 0°$) is observed as two crescents with bright spots at the center. By contrast, molecules oriented perpendicular to the optical axis can appear as a bright circle or as a cloverleaf shape, depending on whether their orientation is parallel or perpendicular to the excitation polarization ($\phi = 0°$ or 90°, Fig. 3). Because the relative intensities of the *x*, *y*, and *z* components are in general not equal, the maximum fluorescence emission will vary according to the molecular orientation. This is summarized in Fig. 3, where the expected maximum fluorescence emission for each of the dipole orientations is given relative to that of an *x*-oriented molecule. The values in this figure were corrected for the different collection efficiencies associated with a given dipole orientation [15, 16], assuming that the focusing of the excitation light and the fluorescence collection are done using the same microscope objective.

As is clear from the previous discussion, after recording a scanning image of an immobilized single molecule we can infer some information about its orientation. However, careful examination of the calculated patterns in Fig. 3 demonstrates that this method is not equally sensitive to every molecular orientation. For example, the calculated patterns do not change significantly if we set $\theta = 0°$ and vary ϕ from 0° to 90°. However, the patterns do change significantly if both θ and ϕ are close to 90° (Fig. 4), and as such the method is seen to be very sensitive to small changes in orientation around these angles, though in actual measurements this sensitiv-

#79032 - $15.00 USD Received 16 January 2007; revised 28 February 2007; accepted 28 February 2007

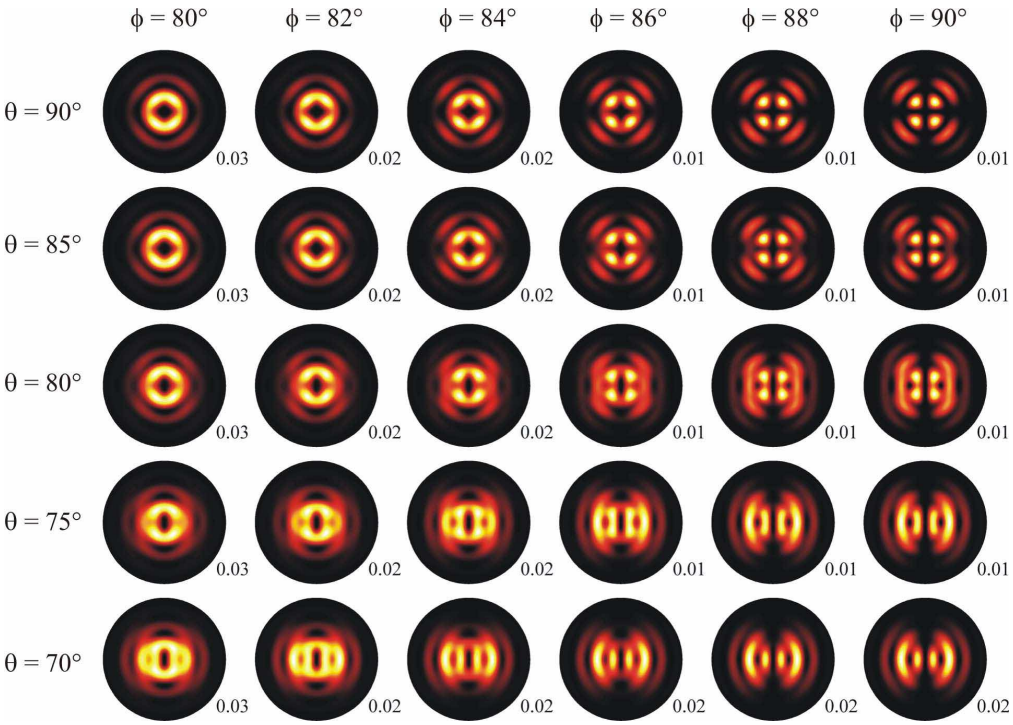

Fig. 4. Expansion of the fluorescence distributions for molecular orientations close to the optical axis of the microscope and perpendicular to the polarization of the input laser beam ($\theta \approx 90°$, $\phi \approx 90°$) The values listed next to the images refer to the maximum observable fluorescence emission for that orientation, relative to that of an *x*-oriented molecule.

ity could be reduced by the rather low expected fluorescence intensities for these orientations (Fig. 4).

Several other techniques for determining the two- or three-dimensional orientation of an immobilized single molecule using far-field microscopy have been proposed and demonstrated. Well-known approaches include the controlled introduction of abberations [17], modulation of the excitation and/or detection polarization [18, 19], (defocused) wide-field imaging [20, 21, 22, 23, 24] and annular illumination [25, 26]. While, for example, defocused widefield imaging retains its sensitivity to the molecular orientation over a wider range of possible orientations, we believe that the present technique is comparatively very sensitive for molecules oriented close to the optical axis of the microscope and roughly perpendicular to the polarization of the excitation light. We thus see that this method has potential for the analysis of single-molecule orientations with high accuracy, but only for a subset of all possible molecular orientations.

3.2. STED microscopy

As we have already mentioned in the introduction, donut modes are extensively used for the realization of light microscopy with sub-diffraction resolution by making use of stimulated emission [27]. This approach is based on the idea that the donut-mode irradiation selectively deactivates only the molecules along the outer edge of the focal volume, while the molecules close to the zero-intensity 'hole' are left to fluoresce spontaneously. Moreover, the dimensions of this hole can in theory be arbitrarily reduced by increasing the intensity of this 'dumping' beam, or, to a certain extent, by increasing its duration. In STED this deactivation is done through

#79032 - $15.00 USD Received 16 January 2007; revised 28 February 2007; accepted 28 February 2007

stimulated emission, and an increased intensity for the dump beam will usually lead to an increased resolution if photobleaching and higher-excited state processes can be avoided [28, 29]. Increasing the duration of the dump beam allows more molecules to be quenched, and can avoid re-excitation of already quenched molecules if this duration is longer than the time required for vibrational relaxation from the vibrationally excited levels of the ground state. However, this duration should not exceed a fraction of the molecule's natural excited state lifetime, as the quenching has to take place before any appreciable fluorescence is emitted.

Stimulated emission, like absorption, is characterized by a well-defined transition dipole moment. Moreover, in many cases the orientation of this transition dipole will be highly similar to that of the associated transition dipole for absorption. The net result is that the probability that a given molecule will be quenched similarly depends not only on its position, but also on its orientation, as has been noted before [30, 31, 32]. Because of the similarity between the processes of absorption and stimulated emission this dependence is similarly given in Fig. 3.

In order to quantify the effect of the molecular orientation on a possible resolution improvement we ran a series of additional simulations. For these simulations we assumed that a large ensemble of molecules with identical orientations is distributed uniformly in a two-dimensional film (equivalently the resulting images can be interpreted as scanning images of a single immobilized molecule), and that the rate of stimulated emission k_{STED} at an arbitrary position is proportional to the intensity of the donut mode beam along the molecule's transition dipole moment. The proportionality constant will be determined by the excited state absorption cross section of the molecule and the probability for stimulated emission, and possibly other factors such as re-excitation of the quenched molecules. Furthermore we assume that the total fluorescence emitted at time t is proportional to the excited state population at t, so that the total amount of fluorescence I that is emitted at every position was then calculated according to

$$I = I_0 \cdot \frac{1}{k_{de-act} + k_{STED}} \{k_{de-act} + k_{STED} \cdot \exp[-(k_{de-act} + k_{STED})\tau]\} \qquad (1)$$

In this equation k_{de-act} is the sum of the rate constants of all processes occurring from the excited state except stimulated emission, I_0 is the total fluorescence emission if no dump beam was applied, and τ is the duration of the dump beam. This equation is based on the assumption that after the excitation of the sample the dump beam is applied immediately, as a square pulse with a characteristic duration τ, and the integration of the resulting excited state population over time.

For the purpose of these simulations we are not interested in absolute populations, STED rate constants, or fluorescence intensities, but rather in the relative differences between the excitation and quenching of molecules at different sample positions and different molecular orientations. In other words, the absolute excited state population and fluorescence at a given position can be scaled by arbitrary (but constant) factors, which simplifies the calculation and allows the results from the diffraction calculation to be used directly. Accordingly we define a 'saturation STED rate constant' k_{STED}^{sat} as the rate constant which leads to a half depopulation of the excited state after being applied for a duration τ, so that k_{STED}^{sat} is given by $\ln 2/\tau$.

Figure 5 shows some results from our calculations. Fig. 5(a) displays the probability that a molecule at a given position in space and with the specified orientation will absorb a photon to form the excited state ('excitation') and the probability that this molecule will be quenched by the dump pulse if it is in the excited state ('dump'), assuming that these states display an identical orientation of the transition dipole moment. As was mentioned before, for the excitation pulse a normal-mode laser beam is assumed, while the dump pulse is modulated into a donut mode. In both of these cases the transition probability depends on the dipole orientation, and both laser beams are assumed to be linearly polarized in the same plane, which we take to be the x-direction.

#79032 - $15.00 USD Received 16 January 2007; revised 28 February 2007; accepted 28 February 2007

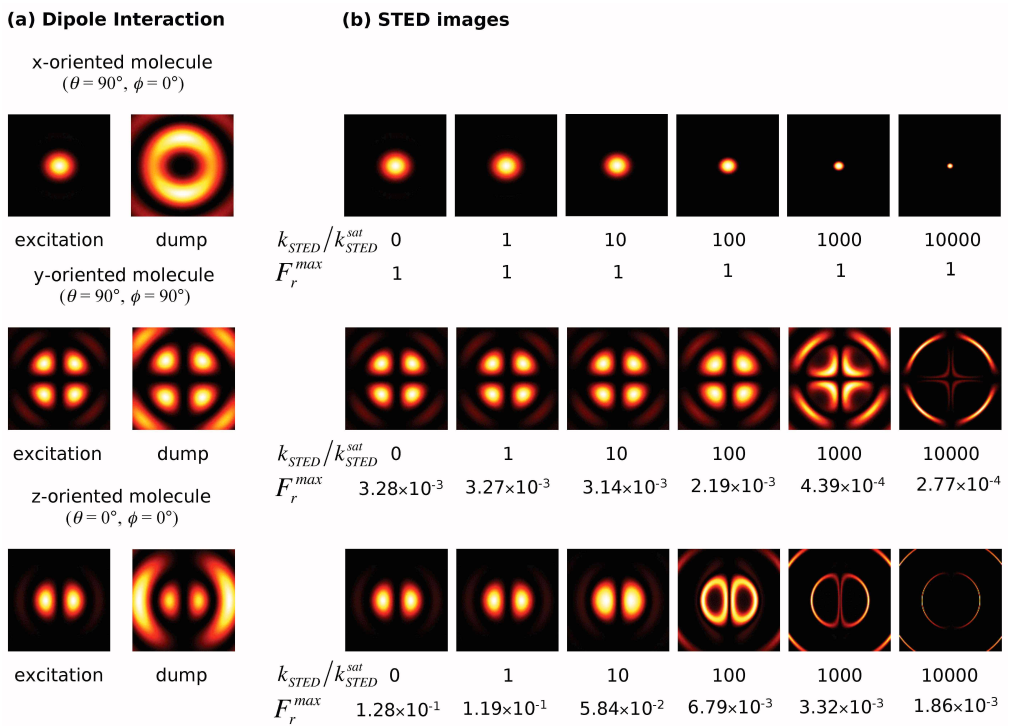

Fig. 5. (a) Simulated dipole interactions for a linearly polarized normal-mode laser beam ('excitation') and donut-mode beam ('dump') for different molecular orientations. (b) Simulated fluorescence distributions obtained for STED measurements at different powers for the dump beam. The molecular orientations corresponds to those in (a). For comparison purposes the relative fluorescence maximum of each image F_r^{max} is given relative to the maximum for normal-mode excitation of an *x*-oriented molecule. Note that the values for F_r^{max} are not corrected for the different collection and detection efficiencies associated with a particular experimental geometry and dipole orientation.

Figure 5(b) shows the expected total generated fluorescence (down to a scaling constant) at each position for a single excitation-dump cycle, which is calculated by combining the calculated dipole interactions and equation (1). The intensity of the applied dump pulse irradiation is proportional to the ratio k_{STED}/k_{STED}^{sat}, which is determined by the maximum value of k_{STED} for each calculation, and the duration of the pulse is taken to be 100 ps. As is clear from Fig. 5, the resulting fluorescence distribution for STED measurements depends extensively on the orientation of the molecular transition dipoles: for an *x*-oriented molecule this distribution is seen to be more or less Gaussian in shape, with a clear increase in resolution as the power of the dump pulse is increased (which is reflected in an increased k_{STED}). By contrast, the images for the *y*- and *z*-oriented molecules show a clearly different picture: unlike the approximately Gaussian distribution of the resulting fluorescence for the *x*-oriented molecule, the fluorescence distribution is seen to correspond to a cloverleaf shape for the *y*-oriented molecule, and a double crescent shape for the *z*-oriented molecule. Moreover the general appearance of these patterns changes as the power of the dump beam is increased.

Obviously then, a STED measurement using linearly polarized laser beams will lead to a resolution increase for only some molecular orientations, while other molecules will instead

#79032 - $15.00 USD Received 16 January 2007; revised 28 February 2007; accepted 28 February 2007

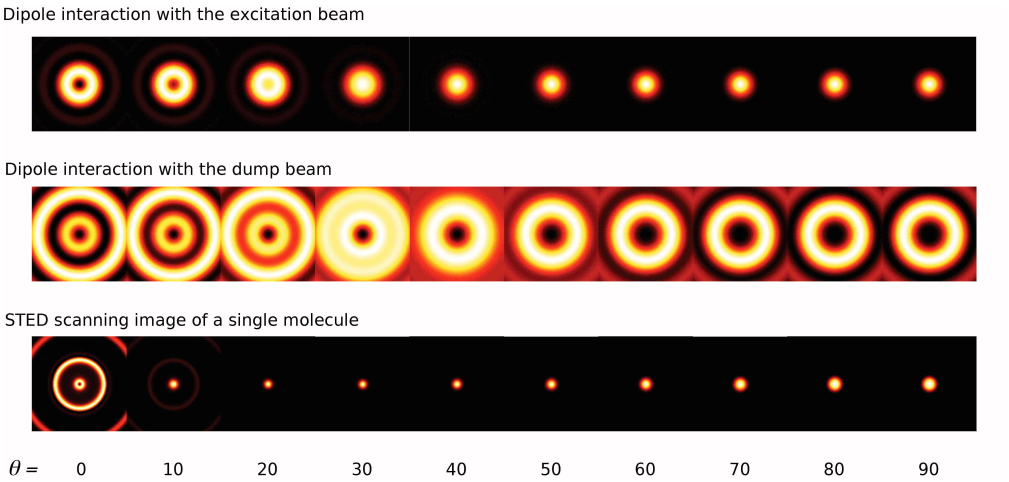

Fig. 6. (Top and Middle) Simulated dipole interactions for molecules at different out-of-plane orientations, using circularly polarized input beams. (Bottom) The resulting simulated STED fluorescence images. In these calculations the ratio of k_{STED} to k_{STED}^{sat} was 100.

contribute in more or less unpredictable ways to the resulting STED image. However, because the intensities of the *y*- and *z*-components are generally less compared to the intensity of the *x*-component, the relative contribution of these 'exotic' patterns will also be less significant compared to the contribution of the *x*-oriented molecules, as shown in Fig. 5(b). However, it is important to realize that the values for F_r^{max} listed in this figure do not take the different collection and detection efficiencies associated with a particular experimental geometry and dipole orientation into account. Thus, using a typical (epifluorescence) setup the recorded emission for a *z*-oriented molecule will be less than can be expected from Fig. 5(b).

In most or all of the actual STED measurements that have been performed both the excitation and dump laser beams are modified to obtain a circular polarization. In this case there is no more dependence of the orientation on the in-plane rotation angle ϕ. However, there is still a dependence on the out-of-plane rotation angle θ, and the results of these calculations are summarized in Fig. 6. In these plots both the dipole interaction of the excitation and dump beam, as well as the resulting STED images are displayed for different molecular orientations, ranging from completely in-plane ($\theta = 90°$) to completely out-of-plane (along the optical axis of the microscope, $\theta = 0°$). The STED fluorescence images once again display a marked dependence on the molecular orientation: for θ ranging from roughly 10° to 90° the images correspond to a central bright spot with weak fringes, while for θ less than 10° the central fluorescence spot splits up into a donut shape with several fringes.

It follows then that the intuitive increase in resolution from STED microscopy is only visible if θ is larger than 10°. Even then, and perhaps counterintuitively, we do not obtain the largest increase in resolution when the molecule is completely in-plane, but rather when θ is close to 21.5°. This is a consequence of the fact that the diameter of the center ring in the donut mode is smaller for the *z*-component of the electric field compared to the in-plane component, even though the intensity of the *z*-component is less than this in-plane component. Moreover, because of the different intensities of each polarization component the different orientations will in general not contribute equally to the emitted fluorescence. These findings are summarized in Fig. 7, where the relative maximum fluorescence emission and the expected resolution are plotted as a function of the out-of-plane angle θ, both for normal-mode and STED microscopy.

#79032 - $15.00 USD Received 16 January 2007; revised 28 February 2007; accepted 28 February 2007

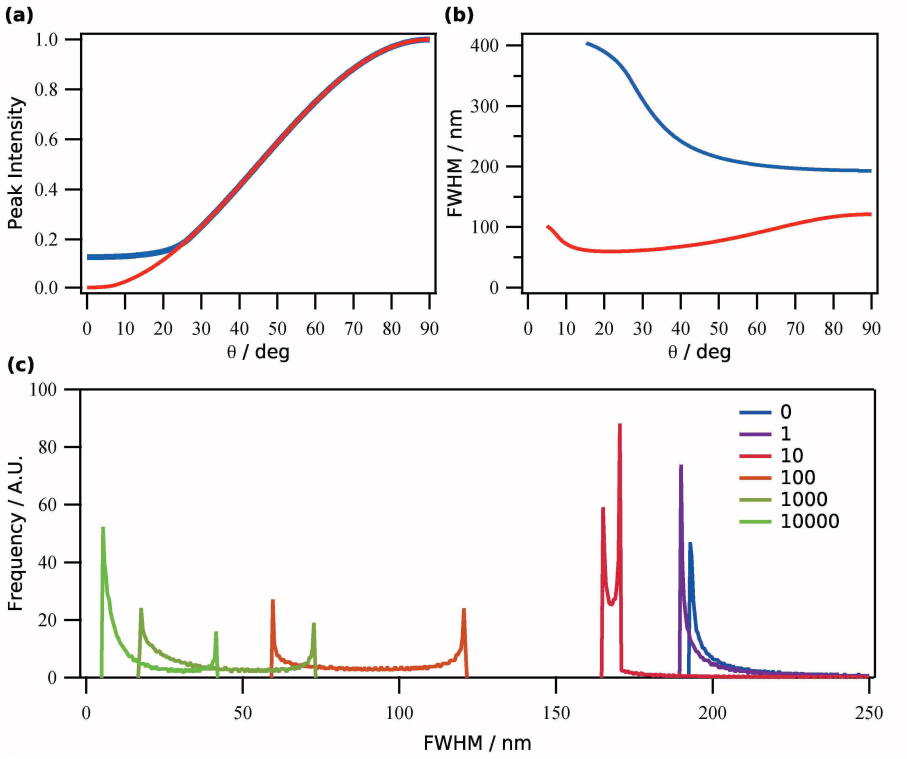

Fig. 7. (a) The maximum fluorescence emission calculated for each simulated STED image as a function of the out-of-plane angle θ, with (red) and without (blue) the dump beam. (b) Expected FWHM of the fluorescence images as a function of θ for measurements with (red) and without (blue) the dump beam. In both of these plots $k_{STED}/k_{STED}^{sat} = 100$. (c) The probability distribution to obtain a certain FWHM (with arbitrary scaling), determined by the probability for a randomly oriented molecule to have its transition dipole moment between θ and $\theta + d\theta$. The values of k_{STED}/k_{STED}^{sat} for each distribution are given in the figure legend.

In this figure we approximate the resolution as the full-width at half maximum (FWHM) of the center bright spot, though we did not estimate the resolution for those cases in which the STED images do not correspond to a central fluorescence maximum. By taking into account the probability that a randomly oriented molecule will have its transition dipole moment between an angle θ and $\theta + d\theta$ we can build up a frequency histogram, which shows the expected distribution of the resolution for randomly oriented molecules at different ratios of k_{STED}/k_{STED}^{sat} (Fig. 7).

It is interesting to note that an analogous dependence on the molecular orientation was found for the precision with which individual fluorophores can be localized in wide-field microscopy [33]. While this technique, and its practical implementation, are fundamentally different compared to STED microscopy, this similarity suggests that the molecular orientation is an important parameter whenever a very high resolution or precision is desired.

#79032 - $15.00 USD Received 16 January 2007; revised 28 February 2007; accepted 28 February 2007

4. Conclusions

In this paper we have discussed the effect of the electric field polarization on the use of donut-mode laser beams. To this end we have calculated a series of simulated images by making use of the vector diffraction theory of light. We find that the use of a linearly polarized donut-mode laser beam for fluorescence imaging can reveal details on the molecular orientation of immobilized single molecules, with a high sensitivity for discriminating molecular orientations close to the optical axis of the microscope and perpendicular to the input polarization.

In a second part of this paper we considered the effect of this polarization on the expected resolution increase in STED microscopy. We find that there is a marked dependence of the resulting STED images of single molecules on the molecular orientation. For linearly polarized laser beams the expected increase in resolution is visible only when the molecules are oriented parallel to the polarization of the laser beams and in-plane ($\phi = 0°$ and $\theta = 90°$). Other orientations generally lead to unexpected patterns, which no longer resemble a bright central fluorescence spot but rather cloverleaf or double-crescent shapes.

To match most experimental conditions we further simulated the effect of molecular orientation in combination with circularly polarized excitation and dump laser beams in STED microscopy. We find that the expected resolution increase depends significantly on the out-of-plane angle θ, and that the increase is at a maximum for θ roughly equal to 21.5°. If the orientation of the single molecule is close to the optical axis of the microscope ($\theta < 10°$) then the resulting fluorescence image no longer corresponds to a central fluorescence spot, so that there is no intuitive increase in resolution. We thus find that there is always a distribution of the resolution improvement for STED measurements, depending on the orientations of the sample molecules.

Acknowledgments

Financial support from the KULeuven research fund (GOA 2/06, Center of Excellence INPAC), the Federal Science Policy of Belgium (Grant IUAP-V-03 and IUAP-VI), the FWO (G.0366.06 and G.0229.07) and from the IWT through ZWAP04/007 is acknowledged. Peter Dedecker is a fellow of the 'Fonds voor Wetenschappelijk Onderzoek' (Aspirant van het FWO). Benoît Muls thanks the 'Fonds de Recherche pour l'Industrie et l'Agriculture' for a fellowship. This work was partially financed by the Impulse Initiative Cell Imaging Core of the K.U.Leuven (via a fellowship to J. Hotta).

#79032 - $15.00 USD Received 16 January 2007; revised 28 February 2007; accepted 28 February 2007